Received: 21 June 2022 | Revised: 1 September 2022 | Accepted: 6 September 2022
DOI: 10.1002/suco.202200604

ARTICLE

fib CEB-FIP WILEY

Reliability-based design of transmission and anchorage lengths in prestressed concrete elements

Flora Faleschini[1,2] | **Lorenzo Hofer**[1] | **Sergio Belluco**[1] | **Carlo Pellegrino**[1]

[1]Department of Civil, Environmental, and Architectural Engineering, University of Padova, Padova, Italy

[2]Department of Industrial Engineering, University of Padova, Padova, Italy

Correspondence
Flora Faleschini, Department of Civil, Environmental, and Architectural Engineering, University of Padova, Padova, Italy.
Email: flora.faleschini@unipd.it

Abstract

This work proposes new reliability-based formulations for the design of transmission and anchorage lengths in prestressed reinforced concrete, starting from the equations discussed and proposed by *fib* TG2.5 "Bond and Material Models." To this end, an extensive experimental dataset with more than 900 results was collected from the scientific literature. Then, two deterministic models were proposed, one for the transmission and one for the anchorage length. For each, model uncertainty was evaluated, and then a probabilistic calibration of their distributions was carried out, separating the cases when sudden or gradual prestress release was applied. Then, probabilistic models were developed for transmission and anchorage length evaluation, depending on the prestress release method: from them, it was possible to evaluate suitable coefficients to target varying reliability indexes. Particularly, two design situations were considered, for transverse stresses verification at the Serviceability Limit State (SLS) and shear and anchorage verification at the Ultimate Limit State (ULS). Lastly, the reliability of current deterministic models was verified.

KEYWORDS

anchorage length, bond, prestressed concrete, reliability, transmission length

1 | INTRODUCTION

In prestressed concrete (PC) elements with pre-tensioned tendons, the global behavior of the members depends on the bond between prestressing steel and concrete. For the correct design of a pretensioned concrete element, two different bond situations should be considered, which depend on the radial deformation of the tendon.[1] Indeed, at prestress release, the radial expansion of the strand due to the Hoyer effect[2] leads to a push-in condition, while, under external loads, a pull-out situation occurs when steel stress increases. These two circumstances identify two different lengths, named transmission (L_t) and flexural bond (L_b) length, respectively. The sum of these two distances represents the anchorage length (L_a), that is, the length over which the ultimate tendon force is fully anchored in the concrete (Figure 1a). Particularly, within the transmission length, stress and strain vary along the strand when the prestress is transferred into

Discussion on this paper must be submitted within two months of the print publication. The discussion will then be published in print, along with the authors' closure, if any, approximately nine months after the print publication.

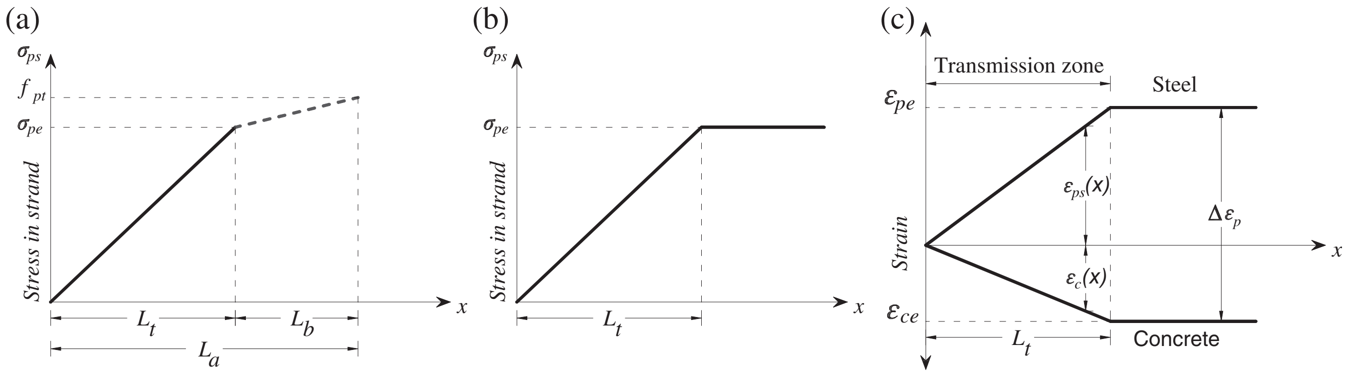

FIGURE 1 Transmission (L_t) and anchorage (L_a) length definition (a); stress profile in the strand (b); and strain profile in the strand and concrete (c)

the concrete. Figure 1b shows that the stress at the member end is null ($\sigma_{ps} = 0$ at $x = 0$), and it gradually increases until reaching the full effective prestress ($\sigma_{ps} = \sigma_{pe}$ at $x = L_t$). This value remains constant or slightly decreases due to long-term effects in absence of external load, even outside the transmission length zone. The same trend is observed for the strain development in both the strand and concrete (Figure 1c). When the prestressing reinforcement is subject to additional stresses due to external actions on the PC member, the stress increases additionally up to the ultimate tensile strength ($\sigma_{ps} = f_{pt}$ at $x = L_a$).

In the design practice, the transmission length L_t is used mainly for the verification of the transverse stresses near the beam ends at the Serviceability Limit State (SLS) or for anchorage length calculation and shear verification at the Ultimate Limit State (ULS). Depending on the design situation, shorter or longer values of the transmission length imply a more onerous verification. Particularly, on one hand, it is necessary to design a sufficient amount of transverse reinforcement to prevent concrete bursting and cracking due to transverse stresses acting in the PC sections. If transverse stresses exceed concrete tensile strength, cracks are developed. The maximum transverse stresses are present at the PC member ends, which gradually reduce along L_t. Thus, overestimating L_t is not recommendable for this design situation, as it reduces the computed value of the transverse stresses acting in one section. On the other hand, if we consider a scheme of simply supported PC elements, shear demand is high at the supports, which distance coincides roughly with the transmission length zone. If the prestress force is not transferred adequately within the required distance from the end of the PC member, the sections placed in this zone may be subject to shear failure. As a consequence, shear cracks may be displayed in this region, which may be originated due to different co-causes, such as poor construction detailing, poor concrete quality, or, as above-cited, wrong transmission length quantification and insufficient shear reinforcement. In this design situation, underestimating L_t is not recommendable as it leads to an unsafe design against shear failure. In fact, it is important to ensure an adequate transmission of the prestress force within a defined distance from the free ends of the strands, where the shear-critical sections are located. The second main design situation where it is fundamental to consider a longer L_t value is linked to the design of the anchorage length L_a.

The current definitions of the transmission and anchorage lengths in design codes are mostly obtained from semi-empirical[3,4] or empirical models.[5] In such models, the direct application of partial safety factors for materials strength does not allow to obtain a coherent level of reliability,[6] leading to potential wrong estimation of the structural reliability, and thus to a non-optimal design. Specifically, assuming shorter or longer values of the transmission length affects multiple design aspects. Moreover, other models can be found in the literature for the computation of the transmission length, employing iterative algorithms based on a modified thick-walled cylinder theory[7,8] or non-linear finite elements.[9,10] However, closed-form expressions are needed to perform the reliability analysis which is the object of this study. Accordingly, in this work, we propose new probabilistic models for the transmission and anchorage lengths starting from the *fib* Model Code 2020 proposal that can be applied to different reliability targets, considering both cases when the prestress force is gradually or suddenly released. From them, specific coefficients can be obtained for each design situation. Among the possible methodologies for the probabilistic calibration of a model,[11–13] we followed the reliability format defined in[14] after a proper assessment of model uncertainties, carried out on an extensive dataset collected within the activities of the *fib* TG2.5 "Bond and Material Models."

TABLE 1 Equations for transmission length design from the main codes

Code	L_t design equation (SI units)
ACI 318-2019[5]	$L_t = \left(f_{pe}/20.7\right) \cdot \phi$ or $L_t = 50 \cdot \phi$
AASHTO[17]	$L_t = 60 \cdot \phi$
fib Model Code 2010[3]	$L_t = l_{bpt} = \alpha_{p1} \cdot \alpha_{p2} \cdot \alpha_{p3} \cdot l_{bp} \cdot \frac{\sigma_{pi}}{f_{ptd}}$ with $l_{bp} = \left(A_{sp} \cdot f_{ptd}\right) / \left(\phi \cdot \pi \cdot f_{bpd}\right)$ and $f_{bpd} = \mu_{p1} \cdot \mu_{p2} \cdot f_{ctd}$
Eurocode 2[4]	$L_t = l_{pt} = \alpha_1 \cdot \alpha_2 \cdot \phi \cdot \sigma_{pm0} / f_{bpt}$ with $f_{bpt} = \mu_{p1} \cdot \mu_1 \cdot f_{ctd}(t)$

2 | TRANSMISSION AND ANCHORAGE LENGTH DEFINITIONS

Bond mechanisms in prestressed concrete consist of adhesion, friction, and mechanical interlocking,[15] leading to high bond strength development in the first part of the anchorage length, where the Hoyer effect takes place. Bond strength depends on many factors, such as concrete tensile strength, the depth of the concrete cover, and the nominal strand diameter.[16] Both transmission and anchorage lengths depend also on strand prestress magnitude and release method,[8] which can be performed either by flame cutting the strands (sudden release) or by gradually releasing the tendons (by using hydraulic jacks, heat annealing, or by sawing through concrete and the steel).

Not always the above aspects are considered in design equations, as is the case of ACI or AASHTO formulations,[5,17] which adopt very simplified equations. Regardless of this evident simplicity, such formulations clearly distinguish how much the magnitude of the bond strength varies between the transmission and anchorage length. Instead, more refined approaches are provided by the *fib* Model Code 2010[3] and Eurocode 2,[4] which include a higher number of variables, both quantitative and qualitative. Table 1 provides the list of the current design equations of transmission length from the main Codes, whereas Table 2 summarizes the main design equations used for the anchorage length calculation.

2.1 | Proposal for *fib* Model Code 2020

For the proposal of the next *fib* Model Code, the authors working within the TG2.5 have proposed two new formulations for evaluating the transmission $L_t = l_{bpt}$ and the anchorage $L_a = l_{bpd}$ length. The new equations do not substantially modify the current approach of *fib* Model Code 2010. Indeed, the transmission length can be still computed as:

$$L_t = l_{bpt} = \alpha_{p1} \alpha_{p2} \alpha_{p3} l_{bp} \frac{\sigma_{pi}}{f_{ptd}} \tag{1}$$

adopting the same coefficients from the previous version. Particularly, recall that α_{p1} considers the type of release, α_{p2} allows to consider the action effect to be verified (i.e., if l_{bpt} is calculated to assess the transverse stresses or to estimate the anchorage length), and finally, α_{p3} depends on the geometry of the tendon. The values of these factors are reported in Table 3. Compared to *fib* Model Code 2010, the main novelty is linked to the definition of the basic anchorage length l_{bp}, that is, the distance necessary to develop the full strength in an untensioned tendon, which depends only implicitly on the bond strength:

TABLE 2 Equations for anchorage length design from the main Codes.

Code	L_a design equation (SI units)
ACI 318-2019[5]	$L_a = L_t + 1/6.9 \cdot \left(\sigma_{pd} - \sigma_{pm,\infty}\right) \cdot \phi$
AASHTO[17]	$L_a = 0.145 \cdot k \cdot \left(\sigma_{pd} - \frac{2}{3}\sigma_{pm,\infty}\right) \cdot \phi$ $k = 1$ or 1.6 depending on the geometry of the pre-tensioned member
fib Model Code 2010[3]	$L_a = l_{bpd} = l_{bpt} + l_{bp} \cdot \frac{\sigma_{pd} - \sigma_{pcs}}{f_{ptd}}$ with l_{bpt} calculated with $\alpha_{p2} = 1.0$
Eurocode 2[4]	$L_a = l_{pt2} + \alpha_2 \cdot \phi \cdot \left(\sigma_{pd} - \sigma_{pm,\infty}\right) / f_{bpd}$ with $f_{bpd} = \mu_{p2} \cdot \mu_1 \cdot f_{ctd}$ and $l_{pt2} = 1.2 \cdot l_{pt}$

TABLE 3 Factors for computing l_{bpt} according to Equation (1) (same as in *fib* Model Code 2010[3]).

Factor	Value	Description
α_{p1}	1.0	For gradual release of the tendons.
	1.25	For sudden release of the tendons.
α_{p2}	1.0	For calculation at ULS of anchorage length and shear capacity. This factor is associated with $l_{i,0.95}$, that is, the 95% fractile of the l_{bpt} probability density function.
	0.5	For verification of transverse stress due to development and distribution of prestress in the anchorage zone. This factor is associated with $l_{bpt,0.05}$, that is, the 5% fractile of the l_{bpt} probability density function.
	0.75	In the proposed probabilistic model.
α_{p3}	0.5	For strands.
	0.7	For indented or crimped wires.

TABLE 4 Factors for computing l_{bp} according to Equation (2) (modified from *fib* Model Code 2010[3]).

Factor	Value	Description
η_{p1}	0.42	For indented and crimped wires.
	0.36	For 7-wire strands.
η_{p2}	1.0	For all tendons with an inclination of 45–90° with respect to the horizontal during concreting.
	1.0	For all horizontal tendons which are up to 250 mm from the bottom or at least 300 mm below the top of the concrete section during concreting.
	0.7	For all other cases.

$$l_{bp} = \gamma_c \frac{A_{sp}}{\pi Ø} \frac{f_{ptd}}{\eta_{p1}\eta_{p2} f_{ck}(t)^{1/2}} \tag{2}$$

Equation (2) includes the partial safety factor for concrete compressive strength γ_c and depends directly on $f_{ck}(t)$, which is the characteristic concrete compressive strength at time t, that is the time of the prestress force release for l_{bpt} calculation. Instead, t is equal to 28 days when l_{bp} is used to calculate the design anchorage length l_{bpd}. The new values assumed by the coefficients η_{p1} and η_{p2} are reported in Table 4.

Lastly, the design anchorage length can be still calculated as:

$$L_a = l_{bpd} = l_{bpt} + l_{bp} \frac{\sigma_{pd} - \sigma_{pcs}}{f_{ptd}} \tag{3}$$

2.2 | Design situations at SLS and ULS

Equation (1) shows that two values for the coefficient α_{p2} (0.5 or 1) can be used to consider the different action effects to be verified. Similarly, Eurocode 2 states that depending on the design situation, the design value of transmission length can be calculated by multiplying l_{pt} by 0.8 or 1.2. In both cases, the Codes define a lower and an upper design transmission length, which roughly represent the fractiles of the probability density function (*pdf*) at 5% and 95%, being $l_{bpt,0.05}$ and $l_{bpt,0.95}$. At each value, implicitly, the Code associates a different bond behavior: in the former case, during the prestress force release, the Hoyer effect significantly contributes and leads to a push-in situation; in the latter case, when the stress in the strand increases under the external actions, the pull-out failure mode governs the mechanical behavior. In this phase, the bond strength developed within the flexural bond length is approximately half of the value in the transmission length. Accordingly, when SLS and ULS verifications should be carried out, different bond strengths need to be considered, and hence, shorter or longer values of the transmission lengths have to be quantified.

2.2.1 | SLS verification: Bursting, spalling, and splitting

Three main transverse stress verifications are required at the end region of a prestressed concrete member, that is, against bursting, spalling, and splitting stresses (Figure 2). Bursting stress occurs due to load spreading, and thus can be associated with a member-level phenomenon; instead, splitting stress occurs due to bond effects, and thus is associated with a local phenomenon, arising in the circumferential area surrounding the tendon. However, in prestressed members, these two phenomena act exactly in the same end region of a member. Spalling stresses act less close to the line of action of the prestress force and are mainly caused by deformation compatibility, prestress eccentricity, or division of the prestress into multiple strand groups.[18] When a combination of these phenomena occurs, cracking may arise being particularly detrimental to the structural integrity of the elements. Often, the cause of these phenomena is an accelerated prestress release, for example, when concrete has not developed enough strength in time.

According to *fib* Model Code 2010,[3] both the bursting and spalling stresses can be evaluated based on a simplified approach using prism models, that is, symmetrical prism according to Guyon theory[19] for bursting and an equivalent prism similar to that proposed by Gergely and Sozen[20] for spalling. The symmetrical prism model adopted for bursting force calculation is shown in Figure 3, where the length of the prism l_{bs}, depending directly on $l_{bpt} = l_{bpt,0.05}$, is given in Equation (4):

$$l_{bs} = \sqrt{h_{bs}^2 + \left(0.6 \cdot l_{bpt}\right)^2} < l_{bpt} \tag{4}$$

The bursting force N_{bs} can be calculated from the moment equilibrium along the section that defines the centroid of the prism A-A, where the internal lever arm z_{bs} is assumed as $0.5 \cdot l_{bs}$:

$$N_{bs} = \frac{0.5 \cdot (n_1 + n_2) \cdot t_2 - n_1 \cdot t_1}{z_{bs}} \cdot \gamma_1 \cdot F_{sd} \tag{5}$$

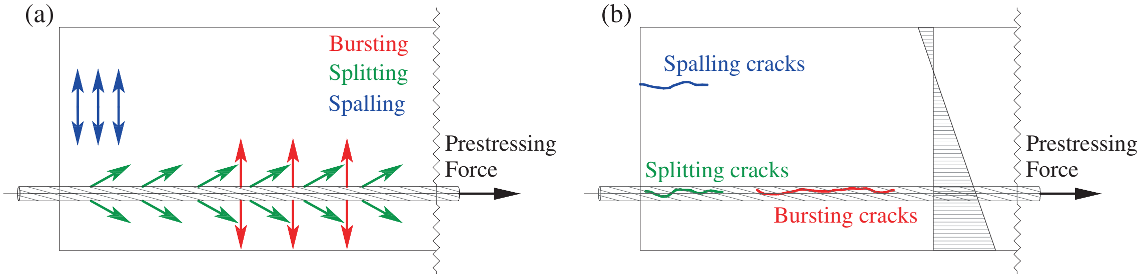

FIGURE 2 Transverse stresses (a) and cracking pattern (b) at the end region of a prestressed concrete member

FIGURE 3 Symmetrical prism model adopted for bursting force calculation

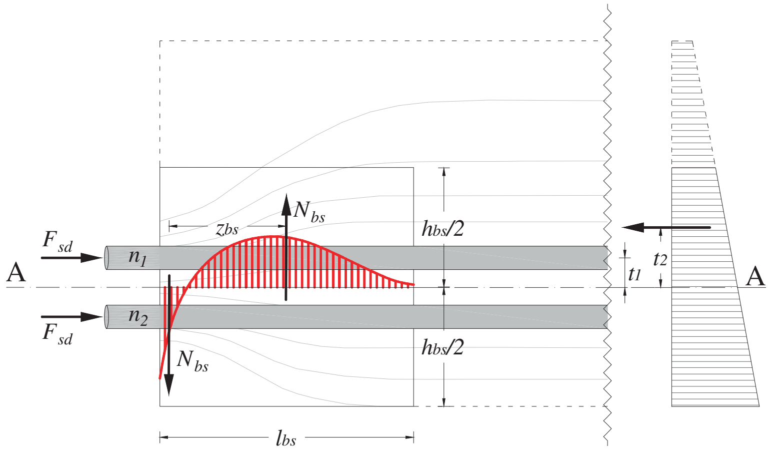

FIGURE 4 Mechanical model for spalling stress computation

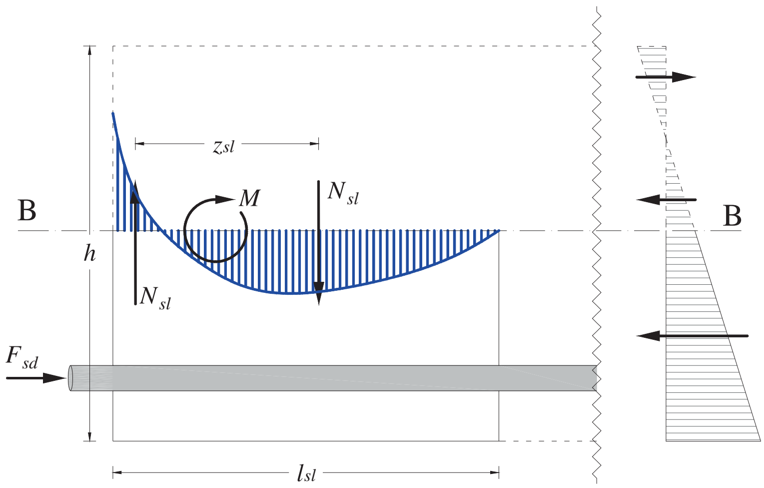

and the bursting stresses σ_{bs} can be obtained by dividing the resulting force by the area of the prism subject to the tensile action, that is:

$$\sigma_{bs} = \frac{2N_{bs}}{l_{bs} \cdot b_{bs}} \tag{6}$$

If the bursting stress exceeds the design tensile strength of concrete f_{ctd}, bursting reinforcement should be designed; conversely, no specific reinforcement is required.

For spalling stresses σ_{sl}, Figure 4 provides the prism geometry, where the equivalent prism length l_{sl} depends again on $l_{bpt} = l_{bpt,0.05}$ and it is computed as:

$$l_{sl} = \sqrt{h^2 + (0.6 \cdot l_{bpt})^2} < l_{bpt} \tag{7}$$

Spalling force is calculated from the moment equilibrium along section B-B in the top portion of the beam, along with no shear force acting, as defined in *fib* Model

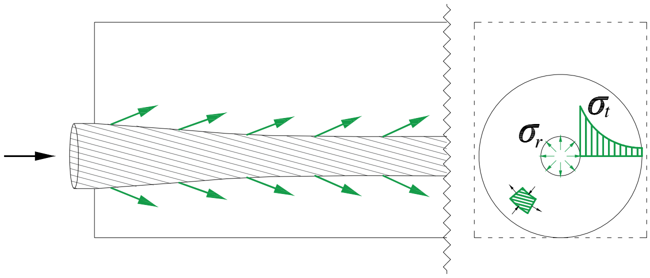

FIGURE 5 Splitting stresses arising at prestress release

Code 1990.[20] Again, the internal lever arm z_{sl} is assumed as $0.5{\cdot}l_{sl}$, to calculate:

$$N_{sl} = \frac{M}{z_{sl}} \tag{8}$$

and the maximum spalling stress is obtained as:

$$\sigma_{sl} = \frac{8N_{sl}}{l_{sl} \cdot b_{sl}} \tag{9}$$

which should be compared with f_{ctd}, and in case of not being verified, it requires the design of proper transverse reinforcement to be put parallel to the end face, in its close vicinity. A simplified graphical approach is provided in the *fib* Model Code 2010 version,[3] where the maximum spalling stress can be obtained as a function of the transmission length and strands eccentricity from the centroid of the beam section, but it is valid for members with height less than 400 mm only. This approach follows a numerical study carried out by Den Uijl.[21] It should be recalled that this verification is particularly restrictive for hollow core slabs, for which EN 1168 standard[22] provides directly a verification equation of the spalling stress:

$$\sigma_{sp} = \frac{P_0}{b_w \cdot e_o} \cdot \frac{15 \cdot \alpha_e^{2.3} + 0.07}{1 + \left(l_{bpt}/e_0\right)^{1.5} \cdot (1.3 \cdot \alpha_e + 0.1)} \tag{10}$$

Equation (10) is based on the same work by Den Uijl,[21] and it depends again on the transmission length $l_{bpt} = l_{bpt,0.05}$.

Lastly, splitting stresses develop circumferentially in reaction to radially directed compressive bond stresses, see Figure 5, thus it should be analyzed as a three-dimensional problem. In a simplified manner, *fib* Model Code 2010 does not provide direct verification of the splitting stresses against f_{ctd}, but it uses a deemed-to-satisfy approach, providing minimum amounts for cover and clear spacing between strands, depending on concrete strength grade.

It should be recalled that *fib* Model Code, as well as other main building codes, allow alternatively the adoption of strut and tie models (S&T) if the stress field has an acceptable complexity to be explicitly modeled, and if a sufficient amount of transverse reinforcement is present to identify the tensed ties. Furthermore, other Codes, for example, AASHTO,[17] propose a single detailing rule for the end-member region, thus superimposing the effects of the multiple transverse stresses acting into a single one.

2.2.2 | Design situations at ULS: Anchorage design, flexural, and shear capacity

At the ULS, the anchorage of prestressing wires and strands should be verified through Equation (3), according to *fib* Model Code 2010. This formulation includes directly $l_{bpt} = l_{bpt,0.95}$, thus assuming a lower bond strength when external actions lead to an increase in the stresses carried by the prestressing reinforcement.

The Code, for providing detailing rules, simplifies Equation (1) for l_{bpt} calculation to be included in Equation (3) for some peculiar cases, that is, for a sudden prestress release and good bond condition for the tendon:

$$l_{bpt0.95} = \begin{cases} 0.10 \cdot \phi \cdot \dfrac{\sigma_{pi}}{f_{ctd}}, & \text{for strands} \\ 0.15 \cdot \phi \cdot \dfrac{\sigma_{pi}}{f_{ctd}}, & \text{for intended wires} \end{cases} \tag{11}$$

Concerning the effects of external action, in both bending and shear strength evaluation, it is important to know how much prestressing force is acting at a given section.[23] Shear verification deserves special attention: indeed, under shear loading, effectively bonded prestressing strands work as a tension tie near supports; if the bond is not fully developed, for example, inside the anchorage length, less tie capacity is obtained. A recent experimental and numerical work has been carried out to analyze the effects of the prestress force in prestressed concrete hollow core slabs, with varying geometry of the webs, showing a complex effect of the varying prestressing force along the end member that may reduce the web-shear resistance.[24] For these specific members, in case of the absence of shear reinforcement, *fib* Model Code 2010[3] provides a design equation for computing the shear resistance of the resisting webs based on an elastic analysis in uncracked conditions:

$$V_{Rd,ct} = 0.8\frac{I_c \cdot b_{w,HC}}{S_c} \cdot \sqrt{{f_{ctd}}^2 + \alpha_1 \cdot \sigma_{cp} \cdot f_{ctd}} \tag{12}$$

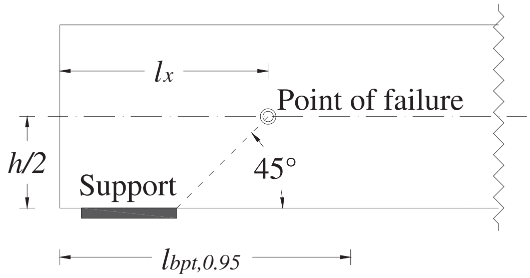

FIGURE 6 Transmission length for ULS design situations

where the reduction factor α_1 identifies the ratio of the distance from the end member to transfer length, and it is typically assumed linear, being $l_x/l_{bpt,0.95}$. For the definition of l_x, generally, the critical section considered for the web-shear strength is fixed at one-half of the slab depth, according to the scheme shown in Figure 6. If Equation (12) is not satisfied, proper transverse reinforcement should be designed.

3 | EXPERIMENTAL DATASET

A dataset comprising 899 transmission lengths and 206 bending tests for anchorage measures has been collected, starting from the existing one collected by Pellegrino et al.,[25] which has been integrated with recently published results available in the scientific literature. Overall, data come from 30 different experimental campaigns described in 35 works, gathered from.[26–61] For each specimen, geometry, material properties, and test methods were reported. From the initial data, a filtering operation was carried out to select a homogeneous sample of specimens that covers only ordinary situations. For instance, the experimental results obtained on specimens with coated or rusted strands were excluded; the same applies to the specimens realized with a concrete grade above C90/105. After this filtering, the dataset includes 598 transmission lengths as experimental measures, whereas the dataset for the anchorage length was not modified. Some characteristics of the specimens belonging to the filtered L_t dataset are summarized below:

i. the mean concrete compressive strength at 28 days ranges between 30 and 89 MPa, while the same value tested at prestress release is between 19 and 76 MPa;
ii. in the majority of the specimens (461 of 598), the applied prestress is around 1375 ± 50 MPa; in the remaining 137 specimens, it ranges from 871 to 1800 MPa;
iii. the employed strands have a nominal diameter between 9.5 and 18.0 mm;
iv. a total of 475 (of 598) measures were calculated with the 95% AMS method,[58] while most of the remaining 123 measures were taken employing the ECADA method[49];
v. more than two-thirds of the specimens were realized performing a sudden release of the strands (425 of 598);
vi. more than 85% of the tested beams (510 of 598) are small-scale specimens, while the remaining 88 are full-scale beams.

Instead, for the L_a dataset, the following considerations can be made:

i. the mean concrete compressive strength at 28 days ranges between 25 and 100 MPa, at prestress release, it is between 21 and 71 MPa;
ii. the initial prestress of the specimens ranges between 871 and 1424 MPa, while the ultimate strength of strands varies between 1655 and 1903 MPa;
iii. the employed strands have a nominal diameter between 6.4 and 15.7 mm;
iv. in about half of the dataset (99 specimens), strands were gradually released, while for the remaining 107, strands were flame cut.

It should be recalled that, from the 206 bending tests analyzed, not all of them provide a single value of the anchorage length: indeed, the evaluation of the anchorage length is an iterative process, where the bending tests are repeated by moving the applied flexural load along the element longitudinal axis, to identify when the failure mode changes from bending/shear to anchorage failure (Figure 7a). Accordingly, from this dataset, it was possible to group the specimens into 41 homogeneous samples to obtain 41 measures: note that only a few of them represent the true L_a value, but in most cases, they identify a lower or upper boundary of the real anchorage length value (Figure 7b,c).

The full and filtered datasets are available at the authors' request, or alternatively, requesting them at the *fib* TG 2.5.

4 | ASSESSMENT OF MODELS UNCERTAINTY

This section shows the procedure adopted to estimate model uncertainty, when analyzing the new formulations

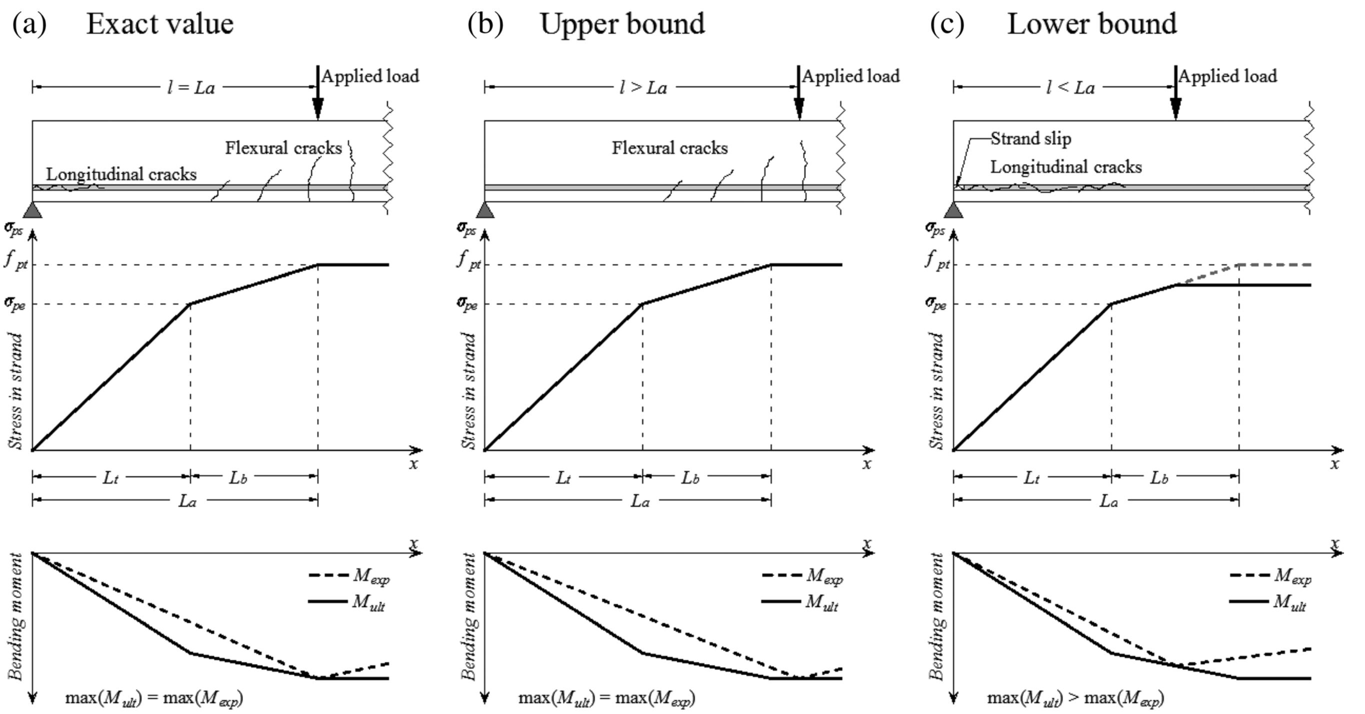

FIGURE 7 Anchorage length estimation procedure based on varying the applied flexural loading point application

proposed by the authors for the forthcoming *fib* Model Code 2020, shown in Section 2.1, to calculate both transmission and anchorage lengths. Specifically, Equations (1) and (3) are the two models analyzed here. The procedure is similar to that used by Mancini et al.[6] within the same *fib* TG works, and in other works by his co-authors.[62,63]

Model uncertainty ϑ is considered as a random variable (*r.v.*), which represents the epistemic uncertainty of the investigated models, and that can be directly evaluated by comparing model to experimental results. As reported in Bairán et al. and JCSS,[13,64] it can be evaluated by means of a multiplicative or an additive relationship. Following the former approach, it is possible to derive the following expression:

$$R(X,Y) \approx \vartheta \cdot R_{mod}(X) \tag{13}$$

where $R(X,Y)$ represents the actual structural response, that is, the one derived from laboratory tests, ϑ is the model uncertainty and $R_{mod}(X)$ is the investigated quantity estimated by the model itself, that is, in this case, using Equations (1) and (3) and the coefficients in Tables 3 and 4. X and Y are two vectors of known and unknown variables, respectively, that can influence the structural response and the modeled result. Note that $R(X,Y)$ is a function of both X and Y, while R_{mod} is a function of only X.

Starting from the *i-th* experimental observations collected from the dataset, a sample of the *i-th* outcomes of ϑ can be computed as:

$$\vartheta_i = \frac{R_i(X,Y)}{R_{mod,i}(X)} \tag{14}$$

where R_i is the actual investigated quantity obtained from laboratory tests, and $R_{mod,i}$ is that estimated by the model. In this work, R_i and $R_{mod,i}$ are substituted, respectively, by l_i and $l_{mod,i}$, which represent the actual transmission (or anchorage) length evaluated from laboratory tests and estimated by the models, respectively.

Figure 8 shows the sample of ϑ_i computed for the transmission (a) and anchorage length (b). Analyzing in detail the values assumed by ϑ_i, a dependency on the prestress force release mode was observed, particularly visible for the anchorage length, even though a proper coefficient was already present in the model equations (coefficient α_{p1} in Equation (1)), as set according to the experimental works by Russel and Burns.[58,59] To remove the dependency on the prestress release mode, two distributions of ϑ were calibrated for each model, obtaining the following combinations: transmission length with gradual prestress release; transmission length with sudden prestress release; anchorage length with gradual prestress release; and anchorage length with sudden prestress release. To this end, the coefficient α_{p1} was removed from Equation (1) (or set at 1, in all cases). After this operation, the independence of ϑ_i from all the other parameters considered by Equations (1) and (3) was verified. Figure 9 shows that the model uncertainty ϑ is independent of the main parameters included in the models, that is, σ_{pi}, $f_{cm}(t)$, ϕ for the transmission length

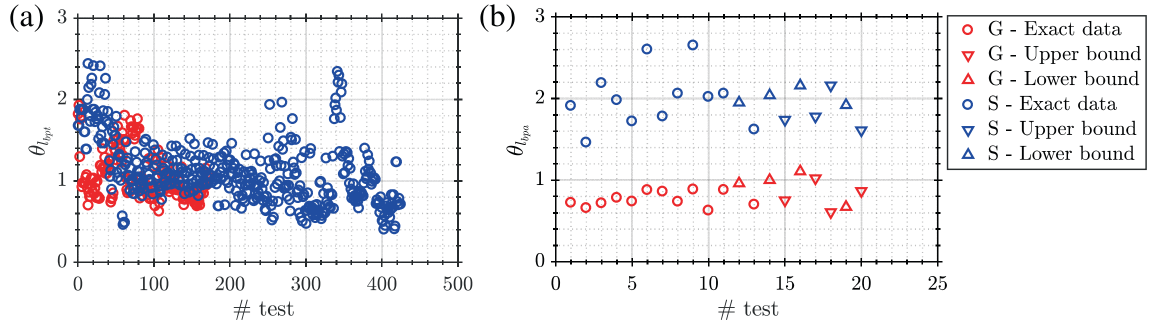

FIGURE 8 Computation of ϑ_i for the transmission (a) and anchorage length (b) for both gradual (G—in red) and sudden (S—in blue) release

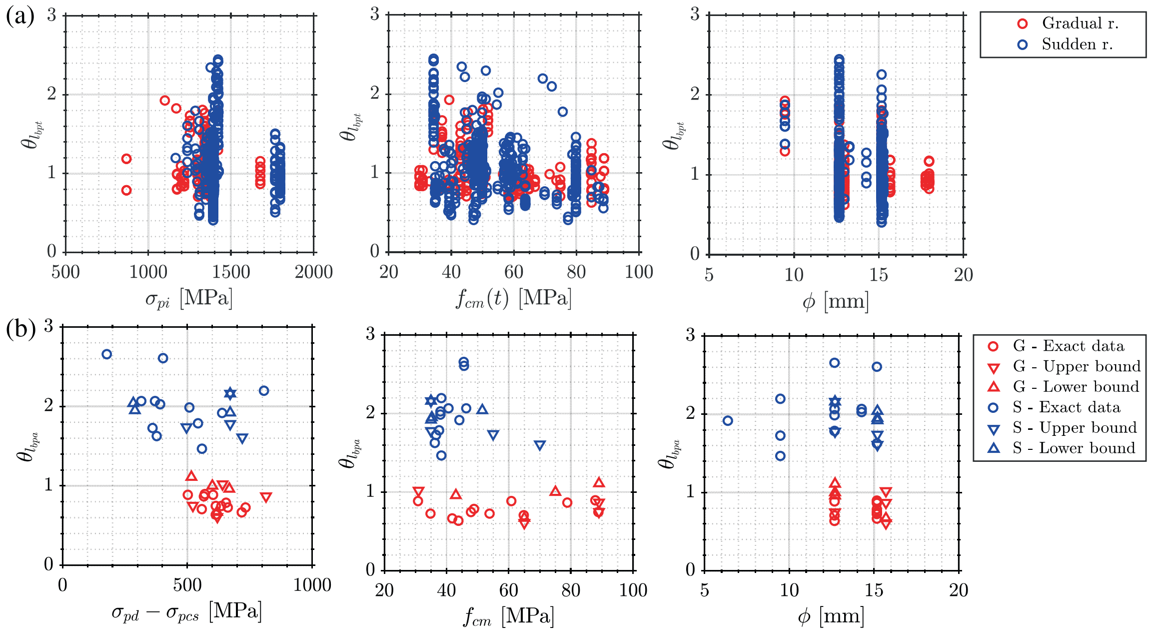

FIGURE 9 Verification of the independency of ϑ on model parameters, respectively, for transmission length (a) and anchorage length (b) for both gradual (G—in red) and sudden (S—in blue) release

(Figure 9a), and $(\sigma_{\mathrm{pd}} - \sigma_{\mathrm{pcs}})$, f_{cm}, ϕ for the anchorage length (Figure 9b). Since no significant trends were found for any parameter in both cases, the statistical characterization of the model uncertainties was performed univocally for all the range of variation of the parameters.

The calibration of the distributions of ϑ for each model was made following two different procedures, one for L_t and one L_a. In fact, the numerousness of the experimental observations is very different in the two cases, and for the anchorage length values, most of the data are censored since the experimental testing procedure is iterative and many times an upper or lower bound is provided, only, as Figure 7 shows. Concerning the ϑ distributions of the transmission length models, the assumptions of normality for ϑ and $ln(\vartheta)$ were verified by means of a Chi-square goodness-of-fit test, with a significance level $\alpha = 0.05$. Figure 10 shows that the hypothesis of normality for ϑ is not verified, while the same hypothesis for $ln(\vartheta)$ is not rejected. In agreement with JCSS,[64] and according to this result, we assumed that the most likely probabilistic distribution for model uncertainties of the transmission length is the lognormal one. Then, the expected value and the standard deviation for both distributions of transmission length (with the gradual or sudden release of prestress force) are estimated with the Bayesian inference procedure, assuming a non-informative prior distribution, according to Gelman et al. and Engen et al.[65,66] The results, in terms of mean value μ_ϑ, standard deviation σ_ϑ, and coefficient of variation δ_ϑ, are reported in Table 5. Results show that the prediction of transmission length is quite accurate for both the gradual and sudden release cases, in which

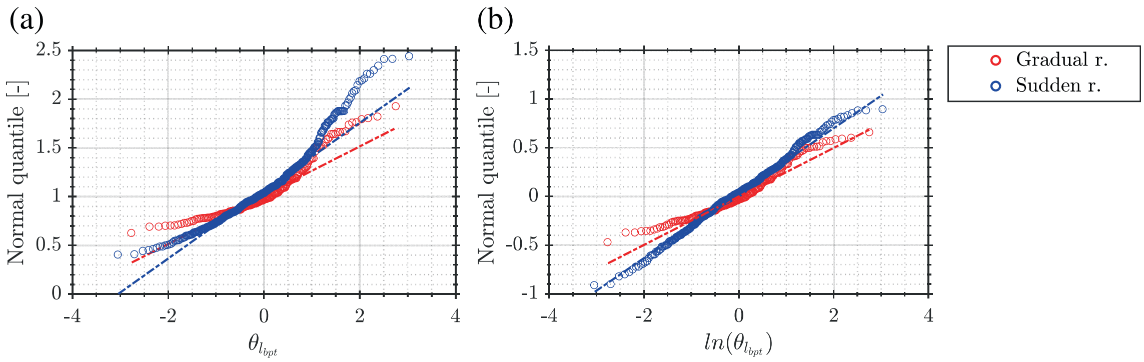

FIGURE 10 Normal probability plot of ϑ (a) and $ln(\vartheta)$ (b) for the transmission length for both gradual (G—in red) and sudden (S—in blue) release

TABLE 5 μ_ϑ, σ_ϑ, and δ_ϑ of the model uncertainty distributions, for the two resistance models and prestress release methods.

	Transmission length		Anchorage length	
Lognormal distribution	**Gradual release**	**Sudden release**	**Gradual release**	**Sudden release**
μ_ϑ	1.05	1.10	0.81	1.93
σ_ϑ	0.28	0.40	0.17	0.48
δ_ϑ	0.26	0.36	0.21	0.25

expected values are, respectively, 1.05 and 1.10. However, the dispersion associated with sudden release (0.36) is greater than the one associated with gradual release (0.26), as demonstrated by the values assumed by δ_ϑ.

Regarding the ϑ distributions for the resistance models of the anchorage length, it should be recalled that the available experimental dataset is quite limited, and it includes several right and left censored data. Furthermore, the experimental evaluation of this quantity is still a matter of research and scientific discussion, since repeated bending tests are necessary to assess the length at which anchorage failure occurs (Figure 7). As a result, most of the data do not identify exactly the anchorage length, but still provide useful information which can contribute to the dataset. To consider the information carried by these partial data, the maximum-likelihood method (MLE) has been adopted for deriving the distributions of ϑ. In this case, however, the normality test of ϑ and $ln(\vartheta)$ was not verified due to the reduced number of experimental evidence, but we assumed that lognormal distribution applies, both for the gradual and sudden release cases. This assumption, even not verified, seems reasonable to the authors for the following reasons: first, it is the same distribution used for the transmission length, which represents physically one part of the anchorage length; then, many works on model uncertainty assessment have used the same distribution for ϑ applied to resistance models for reinforced concrete and bond mechanisms.[6,64] Results, again in terms of μ_ϑ, σ_ϑ, and δ_ϑ, are reported in Table 5, together with those of transmission length. It is worth mentioning that when the sudden prestress release applies, the resistance model significantly underestimates the experimental results ($\mu_\vartheta = 1.93$). On the contrary, the anchorage length computed by the model in the case of gradual release seems to be slightly overestimated ($\mu_\vartheta = 0.81$). However, the δ_ϑ of the two distributions is comparable (0.21 and 0.25, respectively, for gradual and sudden release). It should be recalled that this result has a great impact to understand how the manufacturing method affects the anchorage length required by a member: for instance, hollow core slabs that are typically realized with no "cast-end" but only with "dead-end" during strands cutting, with few energy releases than in ordinary sudden prestress release method, may require less anchorage length than the calculated one. This consideration is in line with the results obtained in,[67] which experimental results are not included in the dataset and thus constitute a valid independent comparison.

5 | PROBABILISTIC MODELS DEVELOPMENT

For both transmission and anchorage lengths, only two quantities are assumed to be *r.v.*, whereas all the others are assumed to be deterministic. The first *r.v.* is the

TABLE 6 Equations for $A(t)$ in Equation (14), with $\alpha_{p2}=0.75$ (intermediate between 0.5 and 1).

Transmission length	Anchorage length
$A(t)=\frac{A_{sp}}{\pi\varnothing}\frac{\alpha_{p2}\alpha_{p3}\sigma_{pi}}{\eta_{p1}\eta_{p2}[\beta_{cc}(t)]^{1/3}}$	$A(t)=\frac{A_{sp}}{\pi\varnothing\eta_{p1}\eta_{p2}}\left[\frac{\alpha_{p2}\alpha_{p3}\sigma_{pi}}{[\beta_{cc}(t)]^{1/3}}+(\sigma_{pd}-\sigma_{pcs})\right]$

concrete compressive strength f_c, which follows a lognormal distribution with a mean value f_{cm} and coefficient of variation $\delta_{f_c}=0.15$.[64] The second *r.v.* is the model uncertainty ϑ, described by a lognormal distribution with μ_ϑ and δ_ϑ, which values are reported in Table 5 according to the present study. Note that the relatively high value of δ_{f_c} represents the variability of the cast in place concrete members, while in laboratory conditions or for the precast concrete subject to factory controls, δ_{f_c} may result in lower values ($0.05\div0.06$). However, to the end of this study, the choice of adopting the largest δ_{f_c} value seems a precautionary and reasonable assumption.

The probabilistic models of the two lengths are derived following the same procedure, starting from Equation (1) or Equation (3), in the case of transmission (l_{bpt}) or anchorage (l_{bpa}) length, respectively. They can be both rewritten as:

$$l_{bpt/bpa}(f_c,\vartheta)=\vartheta\cdot A(t)\cdot f_c^{-\frac{1}{2}} \tag{15}$$

where $A(t)$ represents the multiplicative term grouping all the deterministic parameters of Equations (1) and (3), as reported in Table 6, and derived assuming an intermediate value for $\alpha_{p2}=0.75$. Note that in the remainder of the study, the anchorage length will be indicated by *lbpa* instead of l_{bpd}; the subscript "*d*" will be used for indicating the design length only.

Following the formulation proposed in Taerwe et al.,[14] it is possible to derive a specific quantile q of the lengths' distribution defined in Equation (15) as:

$$l_{bpt,q/bpa,q}=A(t)\cdot\widetilde{\mu}_{f_c}^{-\frac{1}{2}}\cdot\widetilde{\mu}_\vartheta\cdot e^{\Phi^{-1}(q)\cdot\sqrt{ln\left(\delta_\vartheta^2+1\right)+\frac{1}{4}ln\left(\delta_{f_c}^2+1\right)}} \tag{16}$$

where $\widetilde{\mu}_{f_c}$ and $\widetilde{\mu}_\vartheta$ are the median values ($q=0.50$) of the ϑ and f_c distributions, respectively. Since code provisions are usually expressed in function of the characteristic value f_{ck} of the concrete compressive strength, it is particularly useful to re-write Equation (16) as a function of f_{ck} instead of $\widetilde{\mu}_{f_c}$. Since f_c is lognormally distributed, $\widetilde{\mu}_{f_c}$ as a function of f_{ck} can be computed as:

$$\widetilde{\mu}_{f_c}=f_{ck}\cdot e^{-\Phi^{-1}(0.05)\sqrt{ln\left(\delta_{f_c}^2+1\right)}} \tag{17}$$

where q is set equal to 0.05. Substituting Equation (17) in Equation (16), a specific quantile q of the length distribution can be computed in the following way:

$$\begin{aligned}l_{bpt,q/bpa,q}&=A(t)\cdot f_{ck}^{-\frac{1}{2}}\cdot\widetilde{\mu}_\vartheta\\&\quad\cdot e^{\frac{1}{2}\Phi^{-1}(0.05)\cdot\sqrt{ln\left(\delta_{f_c}^2+1\right)}+\Phi^{-1}(q)\cdot\sqrt{ln\left(\delta_\vartheta^2+1\right)+\frac{1}{4}ln\left(\delta_{f_c}^2+1\right)}}\\&=A(t)\cdot f_{ck}^{-\frac{1}{2}}\cdot\zeta_q\end{aligned} \tag{18}$$

where the probabilistic coefficient ζ_q is a function of q, $\widetilde{\mu}_\vartheta$, δ_{f_c}, and δ_ϑ and can be easily computed for each target quantile q as:

$$\zeta_q=\widetilde{\mu}_\vartheta\cdot e^{\frac{1}{2}\Phi^{-1}(0.05)\cdot\sqrt{ln\left(\delta_{f_c}^2+1\right)}+\Phi^{-1}(q)\cdot\sqrt{ln\left(\delta_\vartheta^2+1\right)+\frac{1}{4}ln\left(\delta_{f_c}^2+1\right)}} \tag{19}$$

6 | RESULTS AND DISCUSSION

6.1 | Probabilistic model for transmission length

6.1.1 | Serviceability limit states verifications

In the design practice, the transmission length value is mainly used for SLS verification of the transverse stresses at the beam ends. In this case, the 0.05 quantile is required, since the shorter the transmission length, the more onerous the SLS verification. The transmission length for each desired quantile q can be computed with Equation (18), changing the probabilistic coefficients ζ_q. In this document, only some significant notable cases are reported in Table 7: the median transmission length $l_{bpt,m}$ (with ζ_m, $q=0.50$), the lower characteristic length $l_{bpt,k,0.05}$ ($\zeta_{k,0.05}$, $q=0.05$), and the design length $l_{bpt,d}$ ($\zeta_{d(\beta)}$). The design length $l_{bpt,d}$ can be set as a function of a certain reliability index β, introducing $\Phi^{-1}(q)=\alpha_E\cdot\beta$ in Equation (19), where α_E is the FORM correction factor for the effects of actions, here assumed precautionary equal to -0.7 also at SLS, given the high coefficient of variation of ϑ (Table 5,[3,4,65]). Recall, indeed, that for this verification, the transmission length acts at the action side, whereas the resistance is provided by the tensile strength of the concrete. According to,[4] ζ_d is computed for two target reliability index values, 2.9 for short-term verification (1 year) and 1.5 for long-term verifications (50 years).

The probabilistic models are then applied to an indicative case study to compare their prediction with the deterministic formulation expressed by Equation (1). Hence, a set of given parameters were assumed for both the case of gradual (Figure 11a) and sudden release (Figure 11b): $\phi = 15.2$ mm, $t = 3$ days, $\sigma_{pi} = 1300$ MPa, $\alpha_{p3} = 0.5$, $\eta_{p1} = 0.36$, and $\eta_{p2} = 1$. Overall, Figure 11 shows the values assumed by the transmission length as a function of f_{ck}, evaluated with the probabilistic model from Equation (18) and adopting $A(t)$ from Table 6, depending on the probabilistic coefficients ζ_q selected from Table 7 (i.e., median, lower characteristic and design values for short- and long-term verification). In these graphs, also the transmission length computed with Equation (1) is represented (black line). For the gradual release condition, results demonstrate that the transmission length computed with Equation (1) is close to the ones computed with the probabilistic model associated with a reliability index of 1.5. On the contrary, for the sudden release case, the transmission length computed with Equation (1) is close to the median values predicted by the probabilistic model: this means that, for reaching suitable reliability, comparable to the one obtained for the gradual release, the transmission length should be substantially reduced when sudden prestress method is used. This result is due to the higher uncertainty associated with the sudden release case, as can be easily seen in Figure 11c: indeed, the two cumulated density functions (CDF), calculated varying the q values in Equation (18), have different dispersion. In this example, the variables used for the CDF computation are $f_{ck} = 50$ MPa, $t = 3$ days, and $\sigma_{pi} = 1300$ MPa.

According to this result, it can be confirmed that Equation (1) brings different safety levels if gradual or sudden prestress force release is applied. In the former case, the quantile associated with the transmission length computed with Equation (1) is $q = 0.13$ (corresponding to $\beta = 1.61$), while in the latter the corresponding quantile is $q = 0.396$ (corresponding to $\beta = 0.38$). For the above parameters, aiming to a target reliability index $\beta = 2.9$, the transmission length values provided by the probabilistic models are 339 mm for the gradual and 286 mm for the sudden release cases, against, respectively, 432 mm and 540 mm provided by Equation (1).

Finally, it should be stressed that employing the results of a probabilistic formulation in other models (e.g., those for stress control at the prestressed member end) does not assure the attainment of the same reliability level given by the initial formulation. In fact, it has

TABLE 7 Probabilistic coefficients ζ_q for the transmission length computation at SLS.

	ζ_m	ζ_k	ζ_d	
	$q = 0.5$	$q = 0.05$	$\beta = 1.5$	$\beta = 2.9$
Gradual release	0.90	0.58	0.68	0.52
Sudden release	0.92	0.51	0.63	0.44

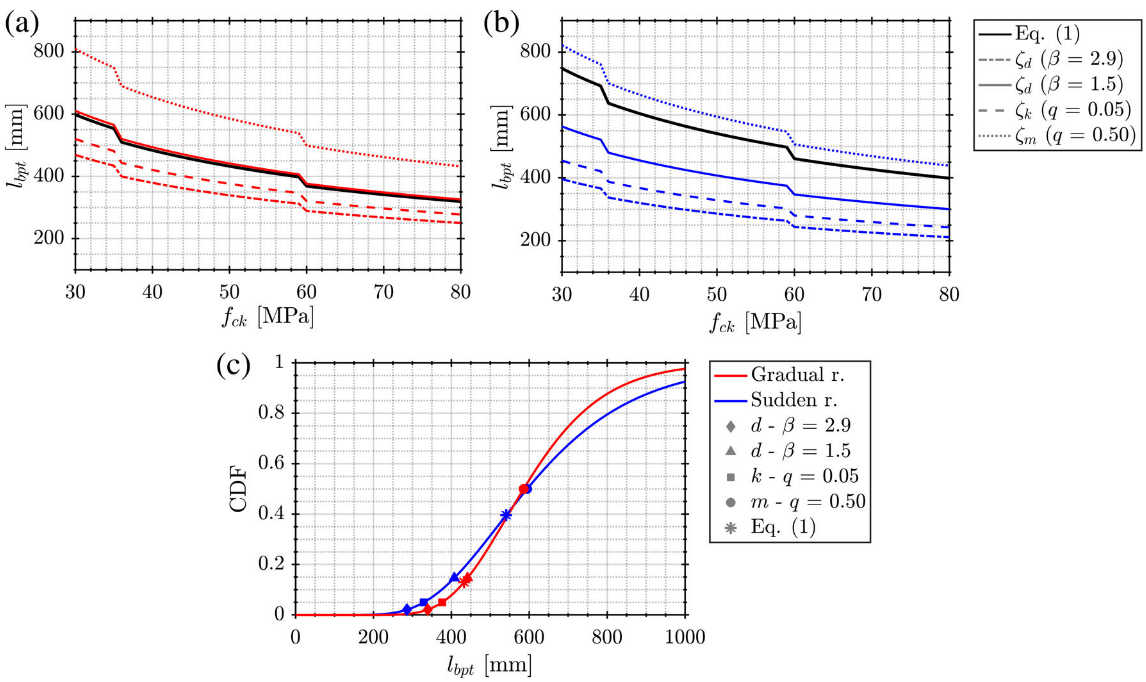

FIGURE 11 Transmission length computation for SLS verifications for gradual (a—red) and sudden (b—blue) release; and transmission length CDFs (c)

been proved that Model Code provisions for bursting and spalling are not always on the safe side,[68] but the reliability evaluation of these aforementioned models is out of the scope of the present study, and further studies linked to the local behavior at the members' ends are necessary.

6.1.2 | Ultimate limit state verification

Other than SLS verifications, the transmission length is also used for shear capacity verification at the ULS. In this case, the 0.95 quantile is required, since the longer the transmission length, the more onerous the ULS verification. As already explained, according to the probabilistic model, the transmission length can be computed with Equation (18) for each desired quantile q, changing the probabilistic coefficients ζ_q. Here, the median transmission length $l_{bpt,m}$ (with ζ_m, $q = 0.50$), the upper characteristic length $l_{bpt,k}$ (with ζ_k, $q = 0.95$), and the design length $l_{bpt,d}$ ($\zeta_{d(\beta)}$) are computed. As previously stated, ζ_d can be set in function of a certain reliability index β, introducing $\Phi^{-1}(q) = \alpha_R \cdot \beta$ in Equation (19), where α_R is the FORM sensitivity factor for resistance. Recall in fact that for this verification the transmission length acts at the resistance side (see Equation (12)), while the action is provided by the shear due to the external forces. According to,[4] for ULS, ζ_d is computed for $\beta = 3.8$ and $\beta = 4.3$, respectively, in case of moderate or high consequence failure, considering $\alpha_R = 0.8$. Table 8 lists the probabilistic coefficients ζ_q for the transmission length computation at ULS.

TABLE 8 Probabilistic coefficients ζ_q for the transmission length computation at ULS.

	ζ_m	ζ_k	ζ_d	
	$q = 0.5$	$q = 0.95$	$\beta = 3.8$	$\beta = 4.3$
Gradual release	0.90	1.40	2.04	2.27
Sudden release	0.92	1.66	2.73	3.16

The probabilistic model for the transmission length evaluation for ULS verification is computed here for a case study, fixing the following variables: $\phi = 15.2$ mm, $t = 3$ days, and $\sigma_{pi} = 1300$ MPa, and considering $\alpha_{p3} = 0.5$, $\eta_{p1} = 0.36$, and $\eta_{p2} = 1$. Figure 12a,b shows, respectively, the results for gradual and sudden release as a function of f_{ck}, where median, higher characteristic, design values for moderate and high consequence failures are shown in color, and the black line represents instead the predictions from Equation (1) (recall, with $\alpha_{p2} = 1$). Particularly, Figure 12a shows that Equation (1) provides very close results to those obtained with the probabilistic model with probabilistic coefficients set for reaching $\beta = 3.8$: the two continuous lines are almost overlapped. Instead, Figure 12b shows that the safety margin is lower. Lastly, Figure 12c shows the transmission length CDFs computed for $f_{ck} = 50$ MPa. Values predicted by

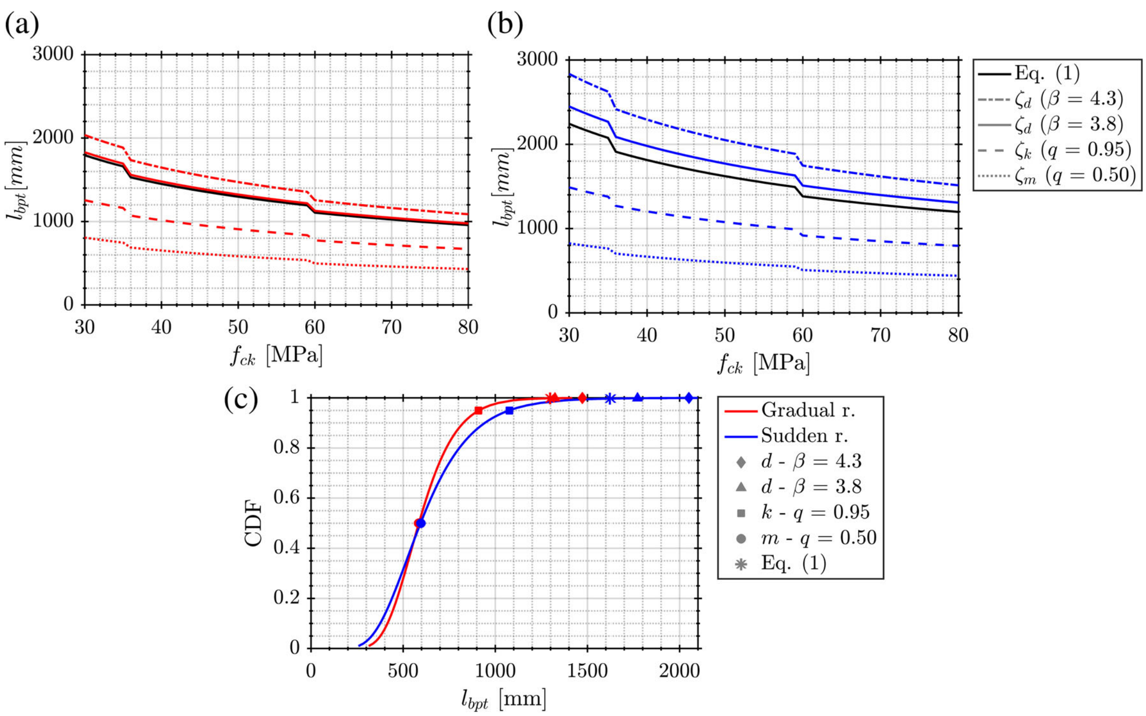

FIGURE 12 Transmission length computation for ULS verification for gradual (a—red) and sudden (b—blue) release; and transmission length CDFs (c)

Equation (1) are 1298 mm and 1623 mm, respectively, for gradual and sudden release, which are associated with $q = 0.9984$ ($\beta = 3.68$) and $q = 0.9974$ ($\beta = 3.49$).

The results obtained here demonstrate again that the deterministic model from Equation (1) is not able to guarantee the same reliability for the two release types; accordingly, transmission length for the sudden release should be increased when ULS verifications have to be carried out.

6.2 | Probabilistic model for anchorage length

The anchorage length is needed for the calculation of the moment and shear capacity of the members at ULS. Thus, the longer the anchorage length, the more onerous the ULS verification. The anchorage length for a specific quantile q can be computed with Equation (18). As done for l_{bpt}, here only some significant notable cases are listed in Table 9: the median length (ζ_m, $q = 0.50$), the upper characteristic (ζ_k, $q = 0.95$), and the design anchorage length ($\zeta_{d(\beta)}$). Similar than in Section 6.1.2, $\zeta_{d(\beta)}$ can be set as a function of a certain reliability index β, introducing $\Phi^{-1}(q) = \alpha_R \cdot \beta$ in Equation (19), where α_R is the FORM sensitivity factor for resistance. According to CEN,[4] $\zeta_{d(\beta)}$ is computed for $\beta = 3.8$ and $\beta = 4.3$, respectively, in case of moderate- or high-consequence failure and considering $\alpha_R = 0.8$. Results are computed fixing the same parameters of the two previous cases, adding $\sigma_{pd} = 1800$ MPa and $\sigma_{pcs} = 1200$ MPa, and are shown in Figure 13a,b, respectively, for the gradual and sudden release case. In both the figures, colored lines are obtained applying the probabilistic models varying the quantile and reliability target, whereas the black line represents the results obtained with the deterministic model from Equation (3). Figure 13a shows that when Equation (3) is applied, it allows achieving a higher reliability index than 4.3, while when the same equation is applied to the sudden release case, the reliability is seriously lower (Figure 13b). The black line lays in fact just between the blue dotted and dashed lines: the anchorage length previsions by Equation (3) are associated with $q = 0.76$, definitively not acceptable for a ULS verification. Figure 13c shows the anchorage length CDFs computed for $f_{ck} = 50$ MPa: from this figure, there is a clear difference in dispersion between the two curves.

TABLE 9 Probabilistic coefficients ζ_q for the anchorage length computation at ULS.

	ζ_m	ζ_k	ζ_d	
	$q = 0.5$	$q = 0.95$	$\beta = 3.8$	$\beta = 4.3$
Gradual release	0.70	1.01	1.37	1.50
Sudden release	1.66	2.52	3.60	3.99

According to these results, it can be affirmed that the reliability level associated with Equation (3) is totally different between the gradual and the sudden release case; for

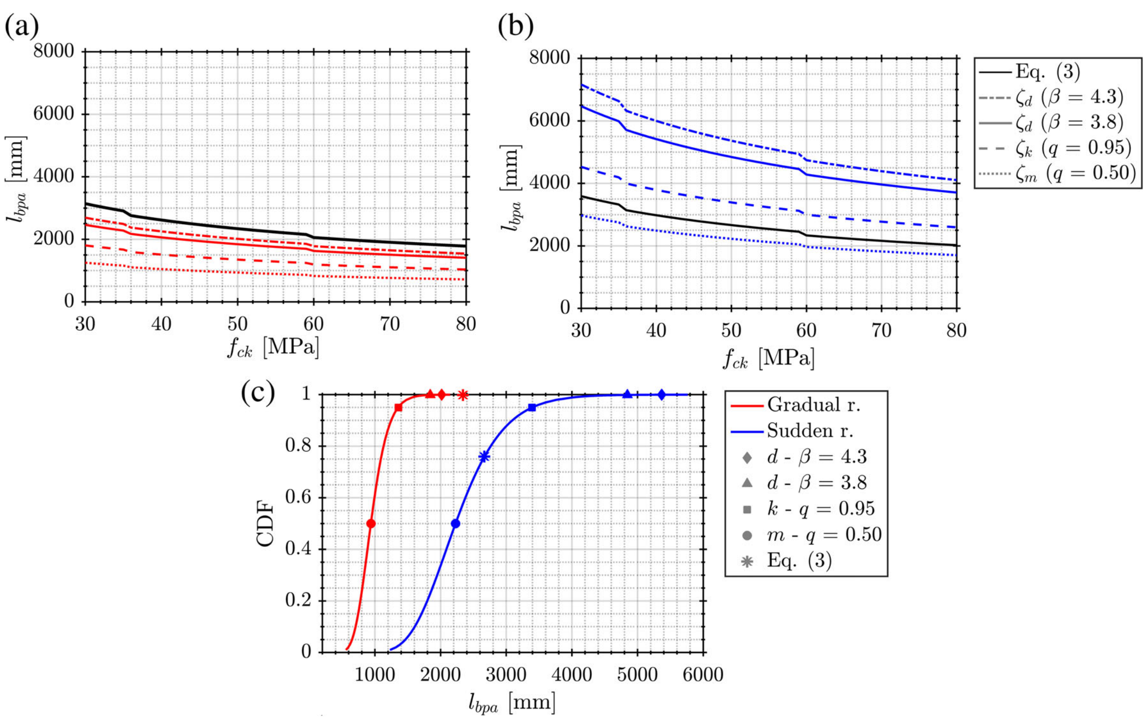

FIGURE 13 Anchorage length computation for gradual (a—red) and sudden (b—blue) release; and anchorage length CDFs (c)

obtaining a comparable safety level, the design length in the case of gradual release should be reduced, while the design length in case of sudden release should be significantly increased.

7 | CONCLUSIONS

Within the *fib* TG2.5 "Bond and Material Models," slight modifications to the current formulations for the design of transmission and anchorage length in prestressed concrete members are currently under discussion. These formulations, reported in Section 2.1 of the present work, were used as a starting point to develop new probabilistic models, shown in Equation (18), where the probabilistic coefficients ζ_q are function of q, $\widetilde{\mu}_\vartheta$, δ_{f_c}, and δ_ϑ and can be easily computed for each target quantile q.

Comparing the predictions from both the deterministic and probabilistic models, within the range of analyzed variables, the following results were achieved:

- adopting the deterministic formulation for the transmission length estimation within SLS verifications, it is not possible to guarantee the same reliability if gradual or sudden prestress release is applied. Particularly, to achieve a target reliability index $\beta = 2.9$, the transmission length values should be shorter than the ones obtained with Equation (1);
- adopting the deterministic formulation for the transmission length estimation within ULS verifications, it is not possible again to guarantee the same reliability if gradual or sudden prestress release is applied. Particularly, the transmission length values obtained with Equation (1) for the sudden release should be larger;
- lastly, adopting the deterministic formulation for the anchorage length estimation, it was demonstrated that the design length in case of gradual release should be reduced, while the design length in case of sudden release should be significantly increased, to achieve the same reliability index.

AUTHOR CONTRIBUTIONS

Flora Faleschini: Conceptualization, methodology, formal analysis, writing (original draft and review), and supervision. **Lorenzo Hofer:** Formal analysis, visualization, and writing (original draft and review). **Sergio Belluco:** Formal analysis, visualization, and writing (review). **Carlo Pellegrino:** Project management, supervision, and writing (review).

ACKNOWLEDGMENT

Eng. Filippo Zattra is gratefully acknowledged for this help during the dataset review and integration.

NOTATION

A_{sp}	Cross-sectional area of the tendon
$A(t)$	Constant in Equation (15), reported in Table 6
b_{bs}	Width of the prism for bursting stresses
b_{sl}	Width of the prism for spalling stresses
b_w	Thickness of the individual web or the total width b of the slab in case of a solid slab
$b_{w,HC}$	Width of the cross-section at the centroidal axis
e_o	Eccentricity of the prestressing steel
f_{bpd}	Bond strength for anchorage in ultimate limit state
f_{bpd}	Design value of the bond strength for prestressing tendons
f_{bpt}	Bond stress at the release of tendons
f_c	Random variable representing the concrete compressive strength
f_{ck}	Characteristic value of the concrete cylindrical compressive strength
f_{cm}	Mean value of the f_c distribution
f_{ct}	Concrete tensile strength
f_{ctd}	Design concrete tensile strength
f_{pt}	Ultimate tensile strength at $x = L_a$
f_{ptd}	Design tendon strength
F_{sd}	Design force per tendon
f_{se}	Effective prestress after all losses (MPa)
h	Section height
h_{bs}	Height of the prism for bursting stresses
I_c	Second moment of area
k	Core radius taken equal to the ratio of the section modulus of the bottom fiber and the net area of the cross-section (W_b/A_c)
L_a	Anchorage length
L_b	Flexural bond length
l_{bp}	Basic anchorage length
l_{bpa}	Anchorage length as addressed in the current paper
l_{bpd}	Design anchorage length of a pre-tensioned prestressing tendon
$l_{bpt,0.05}$	5% quantile of the l_{bpt} distribution
$l_{bpt,0.95}$	95% quantile of the l_{bpt} distribution; l_{bpt} Transmission length of a pre-tensioned tendon
l_{bs}	Length of the prism for bursting stresses
$ln(-)$	Natural logarithm
l_{pt}	Basic value of the transmission length
l_{pt2}	Upper design value of transmission length computed as $l_{pt2} = 1.2 \cdot l_{pt}$
l_{sl}	Length of the prism for spalling stresses
L_t	Transmission length
l_x	Distance from the beam end: generally, the critical section considered for the web-shear strength is fixed at one-half of the slab depth

M Moment given by the concrete stresses above section B-B for spalling stresses
M_{exp} Experimental bending moment depending on the location of the applied load
M_{ult} Ultimate resistant bending moment
n_1, n_2 Numbers of tendons above and below section A-A for bursting stresses
N_{bs} Bursting force
N_{sl} Spalling force
P_0 Initial prestressing force just after release in the considered web or the total prestressing force of the slab in case of solid slabs
q Quantile of the l_{bpt} and l_{bpa} distribution
$R(X,Y)$ Actual structural response derived from laboratory tests
$R_{mod}(X)$ Response estimated by the model
S_c First moment of area above and about the centroidal axis
t_1 Distance between the centroid of tendons above section A-A to the centroid of the prism for bursting stresses
t_2 Distance between the centroid of the concrete stress block above section A-A to the centroid of the prism for bursting stresses
$V_{Rd,ct}$ Design shear resistance for single-span prestressed hollow core slabs without shear reinforcement
X Vector of known variables
Y Vector of unknown variables
z_{bs} Internal lever arm of the bursting forces
z_{sl} Internal lever arm of the spalling forces
α_1 Coefficient considering the type of release (1 for gradual release; 1.25 for sudden release)
α_2 Coefficient considering the type of prestressing tendon (0.25 for tendons with circular cross-section; 0.19 for 3- and 7-wire strands)
α_E FORM correction factor for the effects of actions
α_R FORM correction factor for the resistance
α_e Can be computed as $(e_o - k)/h \geq 0$
α_{p1} Coefficient considering the type of release (Table 3)
α_{p2} Coefficient considering the action effect to be verified (Table 3)
α_{p3} Coefficient considering the influence of bond situation (Table 3)
β Reliability index
γ_1 Supplementary safety factor against overstressing equal to 1.1 for bursting stresses
γ_c Partial safety factor for concrete material properties equal to 1.5
δ_{f_c} Coefficient of variation of the f_c distribution
δ_ϑ Coefficient of variation of the ϑ distribution
ε_c Concrete strain in section x
ε_{ce} Concrete strain at $x = L_t$
ε_{pe} Strand strain at $x = L_t$
ε_{ps} Strand strain in section x
ζ_q Probabilistic coefficient for a specific quantile q or reliability index β (subscript m for median value, k for upper/lower characteristic value, and d for design value)
η_{p1} Coefficient considering the type of prestressing tendon (Table 4)
η_{p2} Coefficient considering the position of the tendon (Table 4)
ϑ Random variable representing the model uncertainty
ϑ_i *i-th* outcome of the random variable ϑ
μ_1 Coefficient considering the bond condition (1 for good bond conditions, 0.7 otherwise, unless a higher value can be justified with regard to special circumstances in execution)—Eurocode 2[4]
μ_{p1} Coefficient considering the type of prestressing tendon (1.4 for indented and crimped wires; 1.2 for 7-wire strands)—*fib* Model Code 2010[3]
μ_{p1} Coefficient that considers the type of tendon and the bond situation release (2.7 for intended wires; 3.2 for 3- and 7-wire strands)—Eurocode 2[4]
μ_{p2} Coefficient considering the position of the tendon (1 for all tendons with an inclination of 45–90° with respect to the horizontal during concreting; 1 for all horizontal tendons which are up to 250 mm from the bottom or at least 300 mm below the top of the concrete section during concreting; 0.7 for all other cases)—*fib* Model Code 2010[3]
μ_{p2} Coefficient that considers the type of tendon and the bond situation at anchorage (1.4 for indented wires and 1.2 for 7-wire strands)–Eurocode 2[4]
$\widetilde{\mu}_{f_c}$ Median value of the f_c distribution
$\widetilde{\mu}$ Median value of the ϑ distribution
μ_ϑ Mean value of the ϑ distribution
σ_{bs} Bursting stresses
σ_{cp} Concrete compressive stress at the centroidal axis due to prestressing, in the area where the prestressing force is fully introduced
σ_{pcs} Tendon stress due to prestress including all losses
σ_{pd} Tendon stress under design load
σ_{pe} Strand full effective prestress at $x = L_t$
σ_{pi} Steel stress just after the release

$\sigma_{pm,\infty}$	Prestress after all losses
σ_{pm0}	Tendon stress just after the release
σ_{ps}	Strand stress in section x
σ_{sl}	Spalling stresses
σ_{sp}	Spalling stresses according to EN 1168[22]
σ_{ϑ}	Standard deviation of the ϑ distribution
ϕ	Strand diameter (mm)
Φ	Cumulative distribution function (CDF) of the standard normal distribution

DATA AVAILABILITY STATEMENT

The data that support the findings of this study are available from the corresponding author upon reasonable request.

ORCID

Flora Faleschini https://orcid.org/0000-0003-2126-9300
Lorenzo Hofer https://orcid.org/0000-0002-2681-696X
Sergio Belluco https://orcid.org/0000-0001-7792-5202
Carlo Pellegrino https://orcid.org/0000-0002-8160-9904

REFERENCES

1. Faria DMV, Lúcio VJ, Pinho Ramos A. Pull-out and push-in tests of bonded steel strands. Mag Concr Res. 2011;63(9):689–705.
2. Hoyer E, Friedrich E. (1939). Beitrag zur Frage der Haftspannung in Eisenbetonbauteilen. Contribution to the issue of detention of iron stress in concrete structures. Beton und Eisen, 38(6), 107–110 (in German).
3. *fib* Model Code. 2010 Lausanne, Switzerland.
4. CEN. Comité Européen de Normalisation. ENV 1992-1-1 Eurocode 2 - Design of Concrete Structures—part 1: general rules and rules for buildings. Brussels: Belgium; 2004.
5. ACI 318-19. (2020). ACI CODE-318-19: building Code requirements for structural concrete and commentary. Farmington Hills, MI, US.
6. Mancini G, Carbone VI, Bertagnoli G, Gino D. Reliability-based evaluation of bond strength for tensed lapped joints and anchorages in new and existing reinforced concrete structures. Struct Concr. 2018;19(3):904–17.
7. Han SJ, Lee DH, Cho SH, Ka SB, Kim KS. Estimation of transfer lengths in precast pretensioned concrete members based on a modified thick-walled cylinder model. Struct Concr. 2016;17(1):52–62.
8. Fabris N, Faleschini F, Pellegrino C. Bond modelling for the assessment of transmission length in prestressed-concrete members. CivilEng. 2020;1(2):75–92.
9. Abdelatif AO, Owen JS, Hussein MF. Modelling the prestress transfer in pre-tensioned concrete elements. Finite Elem Anal Des. 2015;94:47–63.
10. Van Meirvenne K, De Corte W, Boel V, Taerwe L. Non-linear 3D finite element analysis of the anchorage zones of pretensioned concrete girders and experimental verification. Eng Struct. 2018;172:764–79.
11. Faber MH, Sørensen JD. Reliability-based code calibration: the JCSS approach. Applications of Statistics and Probability in Civil Engineering: Proceedings of the 9th International Conference on Applications of Statistics and Probability in Civil Engineering. San Francisco, Californien: Millpress; 2003. p. 927–35.
12. Gardoni P, Der Kiureghian A, Mosalam KM. Probabilistic capacity models and fragility estimates for reinforced concrete columns based on experimental observations. J Eng Mech. 2002;128(10):1024–38.
13. Bairán JM, Tošić N, de la Fuente A. Reliability-based assessment of the partial factor for shear design of fibre reinforced concrete members without shear reinforcement. Mater Struct. 2021;54(5):185.
14. Taerwe RL. (1993), Towards a consistent treatment of model uncertainties in reliability formats for concrete structures. CEB Bulletin d'Information no 219 'Safety and Performance Concepts', 5–34.
15. Janney JR. Nature of bond in pre-tensioned prestressed concrete. J Proc. 1954;50(5):717–36.
16. Martí-Vargas JR, Serna P, Hale WM. Strand bond performance in prestressed concrete accounting for bond slip. Eng Struct. 2013;51:236–44.
17. AASHTO (American Association of State Highway and Transportation). LFRD bridge design specifications. 6th ed. Washington, DC: AASHTO; 2012.
18. Sanders DH. Design and behavior f anchorage zones in post-tensioned concrete members. Dissertation. Austin, TX: The University of Texas at Austin; 1990.
19. Guyon Y. Prestressed concrete. 2nd ed. (English translation) London: F. J. Parsons; 1955. p. 543.
20. Gergely P, Sozen MA. Design of Anchorage Zone Reinforcement in Prestressed concrete beams. PCI J. 1967;12(2):63–75.
21. Den Ujil JA. Tensile stresses in the transmission zones of hollow core slabs prestressed with pretensioned strands [Report]. The Netherlands: Delft University of Technology; 1983. p. 110.
22. CEN. (2012). EN 1168: precast concrete products—hollow core slabs. Brussels, Belgium.
23. Sales MWR, de Araújo Ferreira M, de Lima Araújo D. Evaluation of shear strength of pre-stressed hollow core slab. Structure. 2022;38:1465–82.
24. Nguyen TH, Tan KH, Kanda T. Investigations on web-shear behavior of deep precast, prestressed concrete hollow core slabs. Eng Struct. 2019;183:579–93.
25. Pellegrino C, Zanini MA, Faleschini F, Corain L. Predicting bond formulations for prestressed concrete elements. Eng Struct. 2015;97:105–17.
26. Al-Kaimakchi A, Rambo-Roddenberry M. Measured transfer length of 15.2-mm (0.6-in.) duplex high-strength stainless steel strands in pretensioned girders. Eng Struct. 2021;237:112178.
27. Arezoumandi M, Looney KB, Volz JS. An experimental study on transfer length of prestressing strand in self-consolidating concrete. Eng Struct. 2020;208:110317.
28. Barnes RW, Grove JW, Burns NH. Experimental assessment of factors affecting transfer length. ACI Struct J. 2003;100(6):740–8.
29. Bowser TM, Murray CD, Floyd RW. Bond behavior of 0.6 in prestressing strand in BSCA cement concrete. ACI Struct J. 2020;117(1):43–52.
30. Caro L, Martí-Vargas J, Serna P. Time-dependent evolution of Strand transfer length in pretensioned prestressed concrete members. Mech Time-Depend Mater. 2012;17(4):501–27.
31. Cousins TE, Johnston DW, Zia P. Transfer length of epoxy-coated prestressing strand. ACI Mater J. 1990;87(3):193–203.

32. Cousins TE, Johnston DW, Zia P. Transfer and development length of epoxy coated and uncoated prestressing strand. PCI J. 1990;35(4):92–103.
33. Cousins TE, Johnston DW, Zia P. Development length of epoxy-coated prestressing strand. ACI Mater J. 1990;87(4):309–18.
34. Cousins TE, Stallings JM, Simmon MB. Reduced strand spacing in pretensioned, prestressed members. ACI Struct J. 1994;91(3):277–86.
35. Emerson J, Ruiz E, Floyd R, Hale W. Transfer and development lengths and prestress losses in ultra-high-performance concrete beams. Transp Res Rec. 2011;2251(1):76–91.
36. Dang CN, Floyd RW, Hale WM, Martì-Vargas JR. Measured development lengths of 0.7 in. (17.8 mm) strands for pretensioned beams. ACI Struct J. 2016;113(3):525–35.
37. Dang CN, Floyd RW, Hale WM, Martì-Vargas JR. Measured transfer lengths of 0.7 in. strands for pretensioned beams. ACI Struct J. 2016;113(1):85–94.
38. Dang CN, Hale W, Martí-Vargas JR. Assessment of transmission length of prestressing strands according to *fib* Model Code 2010. Eng Struct. 2017;147:425–33.
39. Dang CN, Martí-Vargas JR, Hale WM. Bond mechanism of 18-mm prestressing strands new insights and design. Struct Eng Mech. 2020;76(1):67–81.
40. Deatherage JH, Burdette EG. Development length and lateral spacing requirements of prestressing strand for prestressed concrete bridge girders. PCI J. 1994;39(1):70–83.
41. Floyd R, Hale W, Howland M. Measured transfer length of 0.6 in. prestressing strands cast in lightweight self-consolidating concrete. PCI J. 2015;60:84–98.
42. Floyd R, Ruiz E, Do N, Staton B, Hale W. Development lengths of high-strength self-consolidating concrete beams. PCI J. 2011; 56:36–53.
43. Hanson NW, Kaar PH. Flexural bond tests of pretensioned prestressed beams. J Proc ACI. 1959;55(1):783–802.
44. Jeon S-J, Shin H, Kim S-H, Park SY, Yang J-M. Transfer lengths in pretensioned concrete measured using various sensing technologies. Int J Concr Struct Mater. 2019;13:43.
45. Kahn L, Dill J, Reutlinger C. Transfer and development length of 15-mm strand in high performance concrete girders. J Struct Eng. 2002;128:913–21.
46. Kim J, Yang J-M, Yim HJ. Experimental evaluation of transfer length in pretensioned concrete beams using 2,400-MPa prestressed strands. J Struct Eng. 2016;142(11):04016088.
47. Kose MM, Burkett WR. Evaluation of code requirement for 0.6 in. (15 mm) prestressing strand. ACI Struct J. 2005;102(3):422–8.
48. Lee S, Shin S, Lee C. Prediction of transfer lengths inclusive of conventional and high-strength strands. J Struct Eng. 2020; 146(9):04020186.
49. Martí-Vargas JR, Arbeláez CA, Serna P, Bugallo MC. Reliability of transfer length estimation from Strand end slip. ACI Struct J. 2007;104(4):487–94.
50. Mitchell D, Cook WD, Arshad A, Tham T. Influence of high strength concrete on transfer and development length of pretensioning strand. PCI J. 1993;38(3):52–66.
51. Mohandoss P, Pillai R, Sengupta AK. Transmission length of pretensioned concrete systems—comparison of codes and test data. Mag Concr Res. 2018;71(17):881–93.
52. Mohandoss P, Pillai R, Sengupta AK. Effect of compressive strength of concrete on transmission length of pre-tensioned concrete systems. Structure. 2020;23:304–13.
53. Oh BH, Kim ES. Realistic evaluation of transfer lengths in pretensioned, prestressed concrete members. ACI Struct J. 2000; 97(6):821–30.
54. Oh BH, Lim SN, Lee MK, Yoo SW. Analysis and prediction of transfer length in pretensioned, prestressed concrete members. ACI Struct J. 2014;111(3):549–60.
55. Oh BH, Sung Kim E, Cheol Choi Y. Theoretical analysis of transfer lengths in pretensioned prestressed concrete members. J Eng Mech. 2006;132(10):1057–66.
56. Over RS, Au T. Prestress transfer bond of pretensioned strands in concrete. J Proc ACI. 1965;62:1451–60.
57. Ramirez-Garcia AT, Floyd RW, Hale WM, Martì-Vargas JR. Influence of concrete strength on development length of prestressed concrete members. J Build Eng. 2016;6:173–83.
58. Russell BW, Burns NH. Measured transfer lengths of 0.5 and 0.6 in. strands in pretensioned concrete. PCI J. 1996;41(5): 44–65.
59. Russell BW, Burns NH. Measurement of transfer lengths on pretensioned concrete elements. J Struct Eng. 1997;123(5):541–9.
60. Shahawy M. A critical evaluation of the AASHTO provisions for strand development length of prestressed concrete members. PCI J. 2001;46(4):94–117.
61. Staton B, Do N, Ruiz E, Hale W. Transfer lengths of prestressed beams cast with self-consolidating concrete. PCI J. 2009;54: 64–83.
62. Gino D, Castaldo P, Giordano L, Mancini G. Model uncertainty in non-linear numerical analyses of slender reinforced concrete members. Struct Concr. 2021;22(2):845–70.
63. Castaldo P, Gino D, Bertagnoli G, Mancini G. Resistance model uncertainty in non-linear finite element analyses of cyclically loaded reinforced concrete systems. Eng Struct. 2020;211:110496.
64. JCSS. Probabilistic model code. Lyngby, Denmark: Joint Committee on Structural Safety; 2001.
65. Gelman A, Carlin JB, Stern HS, Dunson DB. Bayesian data analysis. 3rd ed. London: CRC Press; 2014.
66. Engen M, Hendriks MA, Köhler J, Øverli JA, Åldstedt E. A quantification of the modelling uncertainty of non-linear finite element analyses of large concrete structures. Struct Saf. 2017; 64:1–8.
67. Elliott KS. Transmission length and shear capacity in prestressed concrete hollow core slabs. Mag Concr Res. 2014; 66(12):585–602.
68. Van Meirvenne K, Taerwe L, Boel V, De Corte W. (2016). Verification of the bursting and spalling formulas in the FIB model code by finite element analyses of anchorage zones of pretensioned girders. (Conference title) *fib Symposium 2016*.

AUTHOR BIOGRAPHIES

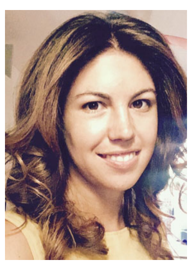

Flora Faleschini,
Department of Civil, Environmental, and Architectural Engineering, University of Padova, Padova, Italy.
flora.faleschini@unipd.it

Lorenzo Hofer, Department of Civil, Environmental, and Architectural Engineering, University of Padova, Padova, Italy. lorenzo.hofer@dicea.unipd.it

Sergio Belluco, Department of Civil, Environmental, and Architectural Engineering, University of Padova, Padova, Italy. sergio.belluco@phd.unipd.it

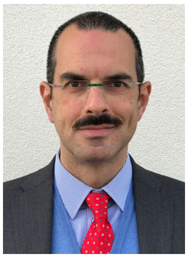

Carlo Pellegrino, Department of Civil, Environmental, and Architectural Engineering, University of Padova, Padova, Italy. carlo.pellegrino@unipd.it

How to cite this article: Faleschini F, Hofer L, Belluco S, Pellegrino C. Reliability-based design of transmission and anchorage lengths in prestressed concrete elements. Structural Concrete. 2022. https://doi.org/10.1002/suco.202200604